Pancreatic Iron: A Future Major Organ in Iron Overload Diseases - The Role of R2*-Relaxometry

Jin Yamamura[1], Sarah Keller[1], Björn Schönnagel[1], Regine Grosse[2], Zhiyue Jerry Wang[3], Peter Nielsen[4], Gerhard Adam[1], and Roland Fischer[1,5]

[1]Diagnostic and Interventional Radiology, University Medical Center Hamburg-Eppendorf, Hamburg, Hamburg, Germany, [2]Pediatric Hematology and Oncology, University Medical Center Hamburg-Eppendorf, Hamburg, Hamburg, Germany, [3]Department of Radiology, University of Texas Southwestern Medical Center, Dallas, Texas, United States, [4]Biochemistry, University Medical Center Hamburg-Eppendorf, Hamburg, Hamburg, Germany, [5]Department of Radiology, Children's Hospital & Research Center Oakland, Oakland, California, United States

Target Audience

Clinicians and scientists dealing with the treatment of rare diseases needing chronic blood transfusions and following excessive body iron accumulation. Especially diseases like Diamond Blackfan Anemia (DBA), Hereditary Hemochromatosis (HHC), and ß-Thalassemia major (TM) in which the MRI can help to measure the iron content by R2* relaxometry.

Introduction/Purpose

In recent years, hepatic and cardiac iron deposition has been studied in detail. Due to its involvement in the development of diabetes - a frequent co-morbidity in iron overload diseases - pancreatic iron should become a field of interest. This study aims to determine the pancreatic iron and fat content in patients with iron overload.

Material and Methods

Patients with transfusion-dependent thalassemia (TDT: n=42) and Diamond-Blackfan anemia (DBA: n=13), hereditary hemochromatosis (HHC: n=11), and healthy controls (CTL: n=14) were studied at our units for clinical liver iron (LIC by biosusceptometry), relative cardiac and pancreatic iron assessment (by MRI-R2*/T2*) by methods outlined in **Figure 1**. Serum lipase and amylase levels were also determined.

Figure 1. Breathhold Magnetic Resonance Spectroscopy (MRS, ***left***) and Chemical Shift Relaxometry (CSR, ***right***) in the **pancreatic tail** of a patient with b-thalassemia major (age: 23 y, in vivo LIC: 900 µg/g_{liver}, ferritin: 350 µg/L, **HOMA = 2.4**). MRS shows the typical fat spectrum also known from the liver (***Hamilton et al, 2010***), CSR shows the oscillating signal pattern with minima / maxima at opposed phase / in phase echo times. (Apparent) Fat Contents (aFC) from CSR ($R2^* = 126\ s^{-1}$, aFC = 48 %) and MRS (T2 corrected FC = 52 %) agreed within their

For assessment of the transversal relaxation rate R2* scans were performed using a breath hold prospective ECG gated (GRE) 2D sequence [12 bipolar echoes, echo time (TE) = 1.3-25.7ms, ΔTE= n·1.16ms, pulse repetition time (TR) = 244ms, flip angle = 20°, bandwidth 1955 Hz/pixel] on a 1.5 T MRI (Siemens AG, Erlangen). A mid-vertebral slice (thickness = 10 mm, pixel resolution 1.25x1.25 mm^2) was selected covering the major part of the liver, spleen, and bone marrow. For the pancreas, a stack of 4-8 of slices without gaps (thickness=5.5mm, pixel resolution 1.25x1.25mm^2). The in vivo liver iron concentration (LIC: dry-weight conversion factor = 6) was measured by biomagnetic liver susceptometry (BLS).

First results at 3.0 T from 3D data acquisition (Philips Medical Systems, Best, The Netherlands) will also be presented and will be intraindividually compared with data from 2D at 1.5 T.

Signal intensity data were assessed by CMRtools (Cardiovascular Imgaing Solutions Ltd). Pancreatic and liver ROI based R2* were determined in the interventricular septum of a mid-papillary short axis slice and in a mid-vertebral slice covering the whole liver. Pancreas signal intensities were averaged from three different ROIs positioned on the tail, body and head of the pancreas.

For a 2-compartment model, the signal intensities S(t) of water protons (w) with no shift relative to its resonance frequency of 126 MHz at 3.0 T (= 0!) and fat protons (f) with a chemical shift (water-fat shift: = 450 Hz or 3.4 ppm) are described by

$S_w(t)=S_w(0)\cdot\exp(-R2_w^*t)$ and $S_f(t)=S_f(0)\cdot\exp(-R2_f^*t)\cdot[\cos(2\pi\nu t)+i\cdot\sin(2\pi\nu t)]$,

with signal amplitudes S(0) and relaxation rates R2*, respectively. The signal intensity (magnitude) image from the MRI scan can be written as, $|S(t)| = |S_w(t) + S_f(t)|$, with terms in the right hand side system given by the real and imaginary components of the above relations. This effective CSR approach results in different relaxation rates $R2_w^*$ and $R2_f^*$ for water and fat, respectively. In the presence of local field distortions by iron we may assume that the relaxation rates for water and fat protons are affected in a similar manner by $R2_w^* = R2_f^*$. Also taking a signal level offset (S_{LO}) into account, the final equation 1 is a robust fit function with 4 free parameters, if = const = 450 Hz. At certain echo times t = TE, the cosinus term will become positive (+1: in phase TE = 4.6, 9.2, … ms) or negative (-1: opposed phase TE = 2.3, 6.9, … ms).

$$(1)\quad |S(t)| = S_w(0)\cdot\exp(-R2_w^*t)\sqrt{\{1+(S_f(0)/S_w(0))^2+2(S_f(0)/S_w(0))\cdot\cos(2\pi\nu t)\}}+S_{LO}$$

An apparent fat content (aFC) can be calculated from the signal amplitudes $S_w(0)$ and $S_f(0)$ by equation 3:

$$(3)\quad aFC = S_f(0) / [S_f(0) + S_w(0)]$$

To obtain the absolute fat content (FC), correction of equation (3) by the longitudinal relaxation rates $R1_w$ and $R1_f$ is needed. This magnitude only approach is limited to the quantification of fat fractions < 50% because of the ambiguity of fat or water dominance, i. e., inter-changing the size of the amplitudes $S_w(0)$ and $S_f(0)$ in equation 1 or 2 will result in the same fit to the signal intensity pattern with complementary fat fractions.

In tissues with no fat infiltration ($S_f(0) = 0$) or overwhelming iron concentration ($S_w(0) >> S_f(0)$), equation 1 or 2 will become the well known mono-exponential model with constant signal level offset (equation 4). This 3-parameter model was fitted to the signal intensities of heart and liver in most patients.

$$(4)\quad |S(t)| = S_w(0)\cdot\exp(-R2_w^*t) + S_{LO}$$

Levenberg-Marquardt algorithm was used to fit the beat frequency pattern.

Statistical analysis:

Linear regression was performed to estimate the relationship between the iron loading in the three different pancreas regions. The relationship between cardiac and pancreatic iron loading as well as hepatic and pancreatic iron loading was estimated by Spearman correlation.

ROC analysis was performed between cardiac and pancreatic R2* to determine how well pancreatic iron served as a surrogate for cardiac iron deposition.

Results

A pancreatic iron gradient from tail to head ($p<10^{-4}$) was found. Median pancreatic R2* rates and aFC (average of tail, body and/or head) for patients with TDT, HHC and DBA differed significantly from controls (see **Figure 2, 3** and ***Pfeifer et al: J Magn Reson Imaging 2014,*** *in press*), highest pancreatic R2* ($211 s^{-1}$) and aFC (36%) were found in the tail region of diabetic patients with TDT. Pancreatic R2* correlated with LIC ($r_s=0.42$, $p=10^{-4}$). Confirming earlier studies, ROC analysis revealed pancreatic R2*, lipase, and amylase being risk parameters for cardiac iron accumulation (pancreatic R2* area: 0.89, $p<10^{-4}$; lipase area: 0.75, $p<10^{-4}$; amylase area: 0.69, $p<10^{-3}$).

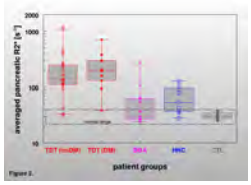

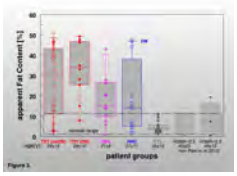

Discussion/Conclusion

Highest iron and fat content was found in the pancreatic tail and pancreatic R2* correlated with cardiac iron deposition. Besides iron accumulation, fatty degeneration might be an additional risk factor for the development of diabetes and might also explain the early onset of diabetes in these patients (see Figure 3). This hypothesis needs further investigation in asymptomatic patients. 3D data acquisition at 3T turns out to be superior to 2D at 1.5 T.